

Constraining Multiphase Gas in Cooling Flows

John S. Arabadjis and Marshall W. Bautz

Massachusetts Institute of Technology

We present a spectral analysis of the central X-ray emission for a sample of galaxy clusters observed with Chandra. We constrain the quantity of a second cospatial temperature component using Markov Chain Monte Carlo sampling and discuss the implications for our understanding of cooling flows.

1. Introduction

The cores of many galaxy clusters are sufficiently dense and cool that the plasma cooling time is shorter than a Hubble time. For many years it was thought that run-away cooling would result in a large central mass deposition rate (Fabian 1994; Allen & Fabian 1997; Peres et al. 1998; White 2000; Allen 2000). Chandra and XMM observations have altered this picture significantly – there appears to be a core temperature floor of 1–2 keV, and inferred mass deposition rates have been reduced by an order of magnitude (Peterson et al. 2001, 2003). Several mechanisms have been proposed to explain the lack of colder gas, including heating by AGN, heat conduction from cluster halo plasma, and small-scale variations in the cooling and metallicity structure of the plasma. Each of these processes can potentially leave a specific observational signature. For example, if conduction provides the energy required to arrest the cooling then the core plasma may be single-phase, but if AGN and/or small-scale inhomogeneities are responsible, one might expect to see observational signatures indicating the presence of multiphase plasma.

We have analyzed a sample of 12 galaxy clusters found in the data archive of the *Chandra X-ray Observatory* for evidence of multiphase plasma in each cluster core. We first describe the method, briefly sketching the Markov Chain Monte Carlo technique, and apply it to a sample of clusters. We then discuss the results and their implications for cooling flows.

2. Method

We use a simple core-halo geometry and Markov Chain Monte Carlo (MCMC) simulations to assess the statistical significance of the presence of multiphase plasma in a sample of clusters. We compare two models of the emission: a simple model M^S which contains one emission component in the halo and one in the core, and a complex model M^C which contains one in the halo and two in the core (see Figure 1).

Each model is fit to a data set consisting of two spectra, one from the outer annulus and one from the inner annulus. Because M^S lies on a boundary of the parameter space of M^C (i.e. the normalization of the second core component goes to zero; Figure 2), the standard F test cannot be used (Protassov et al. 2002). We must instead construct an *empirical* F distribution, using MCMC sampling (sketched below), to which we apply the F test.

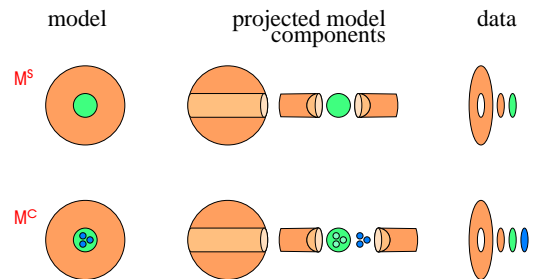


FIG. 1.— Core-halo geometry of the simple and complex models.

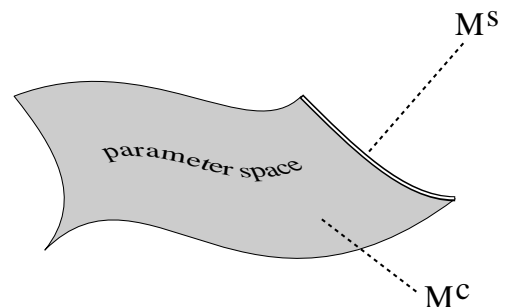


FIG. 2.— Schematic representation of the simple and complex model parameter spaces.

The F statistic,

$$F = \frac{\chi^2(M^S|D) - \chi^2(M^C|D)}{\chi^2(M^S|D)/\nu(M^S)}, \quad (1)$$

is a measure of the improvement in a fit when the simple model is replaced by the complex model. The F distribution of a large number of data realizations allows us to quantitatively compare these two models by comparing the F distribution to the F value of the original data set.

Given the (known) probability distribution function $P(\mathbf{x})$, where \mathbf{x} is the vector of model parameters, we construct an empirical F distribution using MCMC sampling and perform an F test to determine the significance of a second emission component in the core. The entire procedure is as follows:

1. Model the real data set D_0 with M^S using

XSPEC; call the best-fit parameters \mathbf{x}_0^s .

2. Use XSPEC to calculate $P(D_0|\mathbf{x})$ (i.e., the likelihood).
3. Use Bayes' Theorem to calculate $P(\mathbf{x}|D_0)$.
4. Create a large sample of model parameters \mathbf{x}_i^s using a random walk through the parameter space, rejecting each new position which does not meet an acceptance criterion based upon $P(\mathbf{x}|D_0)$. This is the Metropolis algorithm form of the MCMC technique; see Neal (1993). (We also discard all unphysical excursions in parameter space, i.e. where $T < 0$ or $\rho < 0$.) For each \mathbf{x}_i^s , compute a fake data set D_i , including instrumental effects of the *Chandra* telescope and detectors, as well as counting statistics.
5. Fit each M^s and M^c to each D_i .
6. For each pair of models tabulate its F value given by Equation 1.
7. Bin up the set of F values, creating an unnormalized histogram, and compare to the F value of the original data.

In many applications of MCMC sampling one pays special attention to the finite “burn-in” period during which the Markov chain equilibrates. The length of the burn-in phase depends upon the sensibility of the starting point, and the appropriateness of the scale chosen for the proposal probability distribution step. This is not a consideration in our case because we start each MCMC sample at the (already known) peak of the probability distribution function $P(\mathbf{x})$.

In practice this recipe is computationally intensive, not because of any features of the MCMC sampling *per se*, but because each of the faked spectra must be modeled twice. For a sample size of 1000 simulations, XSPEC must simulate 1000 spectra and calculate 2002 sets of best-fit values for the model parameters (including the original data). This fact leads us to simplify the method. First, in order to reduce the modeling time, we have adopted a simplified core-halo geometry. In this scheme the “core” is represented by a single shell (in this case a sphere), while the halo is represented by another shell. Thus M^s contains four parameters, the temperature and density of each of the two shells, while M^c contains six, the additional two parameters representing the temperature and density of a second cospatial emission component in the core. This simplification also greatly improves the numerical stability of the fitting procedure. The algorithm (steps 1–6 above) is implemented in a Tcl script run within XSPEC.

Once we have completed step 7 we can distinguish between the models. The location of the F value of the data within this empirical F distribution contains information regarding the relative merit of M^s and M^c . We define the significance S of the distribution as

TABLE 1. THE 12 CHANDRA CLUSTERS IN THE SAMPLE.

cluster	dM/dt		reference	S ($N = 1000$)
	$(M_\odot \text{ y}^{-1})$			
A1689	$118 \pm_{118}^{375}$		White (2000)	34.2%
A1795	$453 \pm_{90}^{86}$		White (2000)	82.3%
A1835	$683 \pm_{677}^{677}$		White (2000)	48.3%
A1942	$817 \pm_{741}^{118}$		White (2000)	17.6%
A2029	$547 \pm_{81}^{72}$		Allen (2000)	99.8%
A2104	$0 \pm_{0}^{94}$		White (2000)	66.1%
A2204	$984 \pm_{653}^{383}$		White (2000)	99.9%
CL0024	77.0%
HydraA	$264 \pm_{60}^{81}$		Allen (2000)	...
MS1358	$691 \pm_{287}^{348}$		Allen (2000)	63.4%
MS2137	$1467 \pm_{726}^{880}$		Allen (2000)	27.1%
ZW3146	$2228 \pm_{636}^{357}$		Allen (2000)	98.9%

* There are no measurements (nor upper limits) of cooling flow plasma in CL0024 in the literature.

$$s = \frac{\int_0^{F_{data}} N(F) dF}{\int_0^\infty N(F) dF}. \quad (2)$$

The significance $S = 1 - P_f$, where P_f is the probability that the simple model constitutes the better description, and that the F value of the data is this large strictly by chance. Thus, for a one-parameter model, $S = 0.68, 0.90$, and 0.99 may be interpreted as 1, 2 and 3σ detections of the additional component. When discussing the presence of a second emission component in the X-ray data, we adopt 99% as a threshold significance.

3. Application to Chandra Spectra and Clusters

We apply this method to 12 clusters observed with Chandra. All clusters in the sample are fairly round and, with the exception of CL0024, seem to be fairly spherical with no significant amounts of substructure. Ten of these clusters are generally agreed to contain “cooling flows” in their centers, while two of them, CL0024 and A2104, do not. (Allen (2000) derives an upper limit to the cooling rate in A2104.) In each cluster, the core size is defined as the radial extent containing roughly 3000–4000 source photons. Except for Hydra A, all of the clusters in the sample admit a second emission component in this region. (In Hydra A, the best-fit temperature of the second component equals that of the first, rendering an MCMC F -test irrelevant.)

The resulting F distributions for the entire sample are shown in Figure 3. Statistics for each cluster are shown below. We list the cluster, the pre-Chandra/XMM cooling rates from the literature, a reference for this value, and the multiphase plasma MCMC significance.

4. Discussion

Of the 10 cooling flow clusters in the sample, only three of them – A2029, A2204, and ZW3146 – show evidence for multiphase gas in the core, if we adopt $S = 99\%$

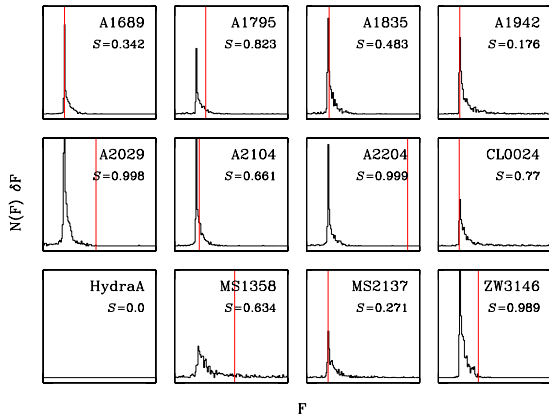


FIG. 3.— Empirical F distributions for the 12 clusters in this study. Note that Hydra A does *not* admit a second core component whose temperature differs from the first.

as our significance threshold. Perhaps more surprising is the fact that the two clusters with the largest pre-Chandra/XMM mass deposition rates – MS2137 and ZW3146 – display such dramatically different evidence for the existence of multiphase plasma. Both were suspected of harboring cooling flows with rates in excess of $1000 M_{\odot} \text{ y}^{-1}$, and yet MS2137 shows no evidence of multiphase gas. (As expected, the two non-cooling flow clusters also show no evidence for a second core emission component.) It could be that, in the absence of recent core merging events, the equilibrium state of the plasma is uniphase, and that the merger and accretion of smaller (and cooler) substructures during the continuing assembly of the cluster are responsible for some clusters showing evidence of multiphase cores. If this were the case, one might look for some evidence for a merging event in MS2137 which has occurred within a cooling time. (As yet we have not found none.) Regardless, it seems that cooling flow cluster cores are an inhomogeneous class.

References

- Allen, S.W. 2000, MNRAS, 315, 269
 Allen, S.W. & Fabian, A.C. 1997, MNRAS, 286, 583
 Fabian, A.C. 1994, ARAA, 32, 277
 Neal, R.M. 1993, Technical Report CRG-TR-93-1, University of Toronto (<ftp://ftp.utoronto.ca/pub/radford/review.ps>)
 Peres, C.B., Fabian, A.C., Edge, A.C., Allen, S.W., Johnstone, R.M. & White, D.A. 1998, MNRAS, 298, 416
 Peterson, J.R., Kahn, S.M., Paerels, F.B.S., Kaastra, J.S., Tamura, T., Bleeker, J.A.M., Ferrigno, C. & Jernigan, J.G. 2003, ApJ, 590, 207
 Peterson, J.R., Paerels, F.B.S., Kaastra, J.S., Arnaud, M., Reiprich, T.H., Fabian, A.C., Mushotzky, R.F., Jernigan, J.G. & Sakelliou, I. 2001, A&A, 365, L104
 Protassov, R. van Dyk, D.A., Connors, A., Kashyap, V.L. & Siemiginowska, A. 2002, ApJ, 571, 545
 White, D.A. 2000, MNRAS, 312, 663